2013 IEEE/RSJ International Conference on
Intelligent Robots and Systems (IROS)
November 3-7, 2013. Tokyo, Japan

Path-generating Regulator along a Straight Passage for Two-wheeled Mobile Robots

Bo Yang, Naohiko Hanajima, Atsushi Yamamoto, Mototada Ayamura and Jun Dai

Abstract— **In this paper, the path-generating regulator is extended to tracking problem along a straight passage for two-wheeled mobile robots. As most of mobile robots are with nonholonomic constraints, it is difficult for us to make them converge to the target state with a control law. To solve this problem, many methods have been proposed. One of them is Path-generating Regulator(PGR) which designs a nonlinear regulator carrying out asymptotic convergence to a given trajectory family. However, the original method is not well suited for passages. In this paper, we will present the extended PGR for the tracking problem along a straight passage. Numerical simulations and experiments are also performed to show the effectiveness of this method.**

I. INTRODUCTION

Path tracking serves as an essential task for autonomous mobile robots. However, most of mobile robots are with nonholonomic constraints[1]. This problem makes it difficult for robots to converge to the target state by deriving a control law[2]. Although many methods focusing on the closed-loop control of nonholonomic systems have been proposed, most of the designed feedback control systems are in chained form which needs input transformation and coordinate transformation. For example, navigation utilizing chained system which is based on local coordinate transformation to the canonical form[3], feedback law based on time-variant analysis[4], [5], quasi-continuous exponential stabilization control[6], discontinuous state feedback control[7], [8], time-state control[9] and nonlinear optimal regulator[10]. A common characteristic of all these discontinuous controllers is that the converting variables can not be defined globally which brings out the result that the feedback control law can not be defined globally as well.

Path-generating regulator(PGR) is a method aimed at controlling mobile robot to move in the tangential direction of the path which passes through the current position of the robot among the path group[11]. The purpose is to make the robot stop at the origin of the rectangular coordinate system fixed to the ground. And the global asymptotic stability of this method for two-wheeled mobile robots has been proved[12].

However, in general, the environment in which mobile robots move is not limited to vast plain. Some closed spaces with certain structures exist as well. Meanwhile, it might be required that the mobile robots move along the given path without stopping at a certain location such as the strawberry harvesting robot moving between two columns of cultivating bench[13] or the internal pipe inspection robot[14]. In these conditions, robots are expected to move along the given straight line without collision against boundaries. It is difficult to apply the original PGR to these conditions as it does not consider the existence of boundaries. In this paper, we propose the extended PGR along a straight passage for two-wheeled mobile robots which keep robots track the given straight line with the consideration of avoiding the collision with boundaries[15].

The line tracking problem of mobile robots has been studied in [16], [17]. A principle which computes the derivative of path curvature as a linear combination of the current vehicle path curvature, vehicle orientation error and positional error was proposed. It successfully found an algorithm for the movement of a robot under the nonholonomic constraints to track a given directed straight line without allowing any spinning motion[16]. Moreover, a path-description method that uses a sequence of straight lines with coordinate transformations for keeping the vehicle moving along a given directed straight line was presented[17]. All of these methods were focused on the way tracking the given directed straight line without considering the boundaries of passages.

This paper is organized as follows. Section II introduces the mathematical model of two-wheeled mobile robot. In section III, the PGR along a straight passage is proposed. Then we apply the proposed PGR to the tracking problem such that a harvesting mobile robot follows the middle of ridge. In section IV numerical simulations and experiments are shown and the properties of the control method are discussed. Section V is conclusion.

II. MATHEMATICAL MODEL OF TWO-WHEELED MOBILE ROBOT

Fig.1 shows the coordinate definition of two-wheeled mobile robot employed in this study. The center point of the axle is set as (x, y). The angle of the robot body axis is set as ϕ which is measured in the counterclockwise direction from the x-axis coordinate. The speed of the robot body axis

Bo Yang is with the Division of Mechanical Systems and Material Engineering, Muroran Institute of Technology, Muroran-shi, Hokkaido, 050-8585 Japan 12052051@mmm.muroran-it.ac.jp

Naohiko Hanajima is with College of Design and Manufacturing Technology, Muroran Institute of Technology, Muroran-shi, Hokkaido, 050-8585 Japan hana@mondo.mech.muroran-it.ac.jp

Atsushi Yamamoto is with the Department of Mechanical, Aerospace and Material Engineering, Muroran Institute of Technology, Muroran-shi, Hokkaido, 050-8585 Japan 2122145@mmm.muroran-it.ac.jp

Mototada Ayamura is with the Division of Mechanical Systems and Material Engineering, Muroran Institute of Technology, Muroran-shi, Hokkaido, 050-8585 Japan 12061059@mmm.muroran-it.ac.jp

Jun Dai is with Division of Production and Information Systems Engineering, Muroran Institute of Technology, Muroran-shi, Hokkaido, 050-8585 Japan s2161014@mmm.muroran-it.ac.jp

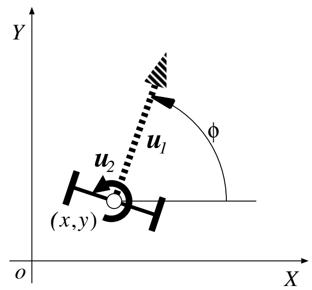

Fig. 1. **State variables and velocity inputs of two-wheeled mobile robot.**

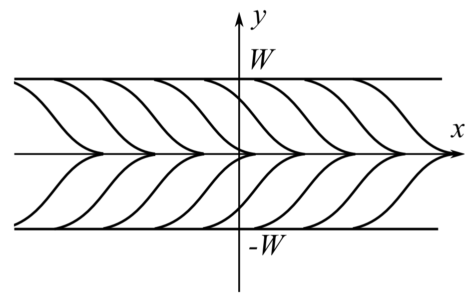

Fig. 2. **Coordinate system and the path functions in the pathway.**

is set as u_1. Since the wheels have no sideslip, the speed in the axle direction is 0. In this condition there is the following non-holonomic bound.

$$\dot{x}\sin\phi - \dot{y}\cos\phi = 0 \tag{1}$$

And the axial velocity of the robot can be expressed as follows.

$$\dot{x}\cos\phi + \dot{y}\sin\phi = u_1 \tag{2}$$

Assuming that the steering angular velocity $\dot{\phi} = u_2$, we can obtain the following mathematical model of two-wheeled mobile robot[11].

$$\dot{x} = u_1 \cos\phi \tag{3}$$
$$\dot{y} = u_1 \sin\phi \tag{4}$$
$$\dot{\phi} = u_2 \tag{5}$$

III. PATH-GENERATING REGULATOR ALONG A STRAIGHT PASSAGE

In this section, the path-generating regulator along a straight passage will be performed.

To illustrate it clearly, we will definite the path function and carry out necessary mathematical calculations firstly, then deduce the steering angular velocity and make an analysis on the moving speed based on the study of stability. Next, the control algorithm of moving speed is proposed. Finally, we will show some extensions of this method.

A. Path Function Definition Along A Straight Passage

We suppose that the robot moves through the center of the passage. The passage is in the form of a space sandwiched between two straight lines. As is shown in Fig.2, the x-axis passes through the center of the passage and the straight lines are set to be $y = \pm W (W > 0)$ as boundaries.

In the region between the x-axis and $y = W$, the following curves which towards the x-axis are used.

$$y = \begin{cases} W & (x < \frac{-\pi+b}{a}) \\ \frac{W}{2}(1-\cos(ax-b)) & (\frac{-\pi+b}{a} \le x \le \frac{b}{a}) \\ 0 & (\frac{b}{a} < x) \end{cases} \tag{6}$$

where a is a positive constant for adjusting the slope of the curve and is related to the maximum value of the target position angle of the mobile robot. Series of the curves can be obtained by any change of the value of b as has been shown in Fig.2. Differentiating y with respect to x and substituting (7),

$$\sin(ax-b) = -\frac{2}{W}\sqrt{(W-y)y} \tag{7}$$

we obtain the slope of the curve expressed as follows.

$$\frac{dy}{dx} = \begin{cases} -a\sqrt{(W-y)y} & (\frac{-\pi+b}{a} \le x \le \frac{b}{a}) \\ 0 & (otherwise) \end{cases} \tag{8}$$

From (8), target angle ϕ_r can be expressed as follows.

$$\phi_r = \tan^{-1}\left(-a\sqrt{(W-y)y}\right) \tag{9}$$

Note that there is no relationship between x and ϕ_r. The partial differentiation of ϕ_r with y is shown as follows, which is used in next section.

$$\frac{\partial\phi_r}{\partial y} = \frac{-a(W-2y)\sqrt{(W-y)y}}{2y[1+a^2(W-y)y](W-y)} \tag{10}$$

As to the region between $y = -W$ and x-axis, the signs of y need to be inverted in (6), (9) and (10).

B. Derivation of Steering Control Based on PGR

The target is to make the robot converge to the x-axis and move along the x-axis at a certain speed. This condition is expressed as $y = 0$, $\phi = 0$. Thus, the control target can be achieved if Lyapunov function of y and ϕ is configured.

The deviation between target angle ϕ_r and the actual angle ϕ is set as δ.

$$\delta = \phi - \phi_r \tag{11}$$

If the following first order system is realized with $\lambda_1 > 0$, the system will be stable.

$$\dot{\delta} = -\lambda_1 \delta \tag{12}$$

Based on (11) and (5), the following expression can be obtained.

$$\dot{\delta} = u_2 - \frac{\partial\phi_r}{\partial y}\dot{y} \tag{13}$$

According to (4), (9) and (13), we set u_2 as follows to satisfy the expression (12).

$$u_2 = -\lambda_1\{\phi - \phi_r\} + \frac{\partial\phi_r}{\partial y}\sin(\phi)u_1 \tag{14}$$

In the region between $y = W$ and x-axis, substituting (9) and (10) we finally obtain

$$u_2 = \begin{cases} -\lambda_1 \phi & (|y| < \epsilon, |y| > W - \epsilon) \\ -\lambda_1 \left\{ \phi + \tan^{-1} \left(a\sqrt{(W-y)y} \right) \right\} & \\ \quad - \frac{a(W-2y)\sqrt{(W-y)y}}{2y[1+a^2(W-y)y](W-y)} \sin(\phi) u_1 & (otherwise) \end{cases} \tag{15}$$

where ϵ is a small positive constant to avoid divergence of u_2.

As to u_2 in the region between $y = -W$ and x-axis, the signs of y need to be inverted in (15).

C. Study of Stability

Suppose that the equilibrium of the robot is that $y = 0$ and $\delta = 0$. A candidate of Lyapunov function $V_1(y, \delta)$ can be set as

$$V_1 = \frac{1}{2} \left\{ \delta^2 + \lambda_2 y^2 \right\} \tag{16}$$

where $\lambda_2 > 0$. Its time derivative is obtained using (4) and (12) as follows.

$$\dot{V_1} = -\lambda_1 \delta^2 + \lambda_2 y \sin(\phi) u_1 \tag{17}$$

Note that (17) is obtained only when $\epsilon < |y| < W - \epsilon$. Now, the space ϕ-y can be divided into four areas.

- Area D_1 : $\phi > 0$ and $y > \epsilon$
- Area D_2 : $\phi < 0$ and $y > \epsilon$
- Area D_3 : $\phi < 0$ and $y < -\epsilon$
- Area D_4 : $\phi > 0$ and $y < -\epsilon$

According to Lyapunov stability theory, if $\dot{V} < 0$ then $|y|$ approaches to ϵ gradually. When $|y| > \epsilon$, δ and ϕ does not become 0 simultaneously. In the case of area D_2 and D_4, $u_1 > 0$ is required. In the case of area D_1 and D_3, u_1 needs to satisfy $u_1 < 0$. When $\phi = 0$, the second term of (17) vanishes. Therefore, $\dot{V} < 0$ is satisfied when $|y| > \epsilon$.

For $|y| < \epsilon$, we set another candidate of Lyapunov function

$$V_2 = \frac{1}{2} \left\{ \phi^2 + \lambda_2 y^2 \right\} \tag{18}$$

where $\lambda_2 > 0$. Its time derivative is obtained using (4) and (15) as follows.

$$\dot{V_2} = -\lambda_1 \phi^2 + \lambda_2 y \sin(\phi) u_1 \tag{19}$$

The sign of u_1 is set to the same manner as V_1. At definition of D_1, D_2, D_3 and D_4, ϵ is needed to be changed to 0. When $\phi = 0$ and $y \neq 0$, we obtain $\dot{V_2} = 0$. Therefore $V_2 \leq 0$ is satisfied. It means that y stays in the neighborhood of 0, however may not converges to 0. Summarizing the above, using the control (15) and choosing the sign of u_1 properly, the robot can approach to x-axis within the range of $|y| < \epsilon$. The value of ϵ can be adjusted as the parameters of the convergence range of y in simulations and experiments.

D. The Control of Moving Speed

As to general path tracking methods, the robots are only required to move forward. Therefore the moving speed u_1 can be any value which matches the condition that $0 \leq u_1 \leq V_m$. Here, V_m is a positive constant representing the maximum speed of the robot. However, as discussed above, if we take the stability into consideration, u_1 has to take a negative value when $y\phi > 0$.

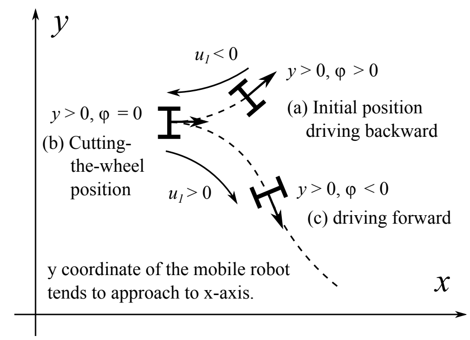

Fig. 3. **Cutting-the-wheel phenomenon.**

Fig.3 shows an example of cutting-the-wheel phenomenon including the condition of $u_1 < 0$. In the initial state (a), the robot satisfies $y > 0$, $\phi > 0$. According to the requirement of stability of the area D_1 $u_1 < 0$. Therefore, the robot begins to move backward along the tangential direction of the path curve and finally reaches the condition (b), when becoming parallel with the x-axis. And ϕ changes from $\phi > 0$ to $\phi = 0$. Then u_1 changes suddenly from $u_1 < 0$ to $u_1 > 0$ when ϕ changes to $\phi < 0$. And the robot begins to move forward towards the x-axis along the path curve. In real passage, since the robot moves backward when $y\phi > 0$, it can avoid the collision with the boundaries of the passage like walls.

A trivial candidate of u_1 considering the stability in the passage is shown as follows.

$$u_1^{stb} = \begin{cases} -V_m & (y\phi > 0) \\ V_m & (y\phi \leq 0) \end{cases} \tag{20}$$

However, u_1^{stb} is discontinuous when the signs of y and ϕ change. It can be changed to a continuous function using the sigmoid function σ_c as follows.

$$\begin{aligned} u_1^{stb\_sig} &= -V_m \left(2\sigma_c(y \sin\phi) - 1 \right) \\ &= -V_m \frac{1 - e^{-cy\sin\phi}}{1 + e^{-cy\sin\phi}} \end{aligned} \tag{21}$$

where c is a positive constant to decide the slope of the sigmoid function. As $y \sin\phi$ has the same signs with $y\phi$, the signs of u_1^{stb} and $u_1^{stb\_sig}$ are the same except when $y\phi = 0$. Since the domain of ϕ is limited to $(-\pi, \pi]$, the sign of ϕ changes discontinuously around $\phi = \pi$. This can be avoided if we choose $\sin\phi$ instead of ϕ.

We also consider a hybrid continuous control algorithm that put more emphasis on advancing around the x-axis and guarantee stability in other places. The control law can be expressed as follows.

$$u_1 = -(1 - K_m e^{-c_m y^2}) \frac{1 - e^{-cy\sin\phi}}{1 + e^{-cy\sin\phi}} V_m + K_m e^{-c_m y^2} V_m \tag{22}$$

where K_m is within the limit of $0 \leq K_m \leq 1$ and $c_m \geq 0$. The first term is used to guarantee the stability and the second term pays attention to go forward. $K_m e^{-c_m y^2}$ is the weighting coefficient to adjust the emphasis between two terms. The value of $e^{-c_m y^2}$ is 1 on the x-axis and approaches to 0 away from the x-axis. c_m is an adjusting parameter. When $K_m = 0$, only the first term will be left and the hybrid control algorithm becomes the same with (21). When $K_m = 1$ and $c_m = 0$, only the second term will be left and it turns to be $u_1 = V_m$.

We show examples to explain the efficiency of u_1 of (22). Set $W = 10$ and $a = 1$ in path function, $\lambda_1 = 1$ in steering angle control algorithm and $c = 1$,$K_m = 1$ $c_m = 1$ in velocity control algorithm. The initial state of the robot is supposed as $x = 0$, $y = 4$, and $\phi = 0$. The trajectories of the robot in 10 seconds are shown in Fig.4. The pentagons represent the location and direction of the robot. The sharp corners are used to represent the direction and the pentagons are drawn every 0.3 second. We can see from the figures that the robot controlled by $u_1^{stb\_sig}$ is trapped in the place where it reaches the x-axis while the robot controlled by u_1 in (22) advances along the x-axis towards the positive direction smoothly.

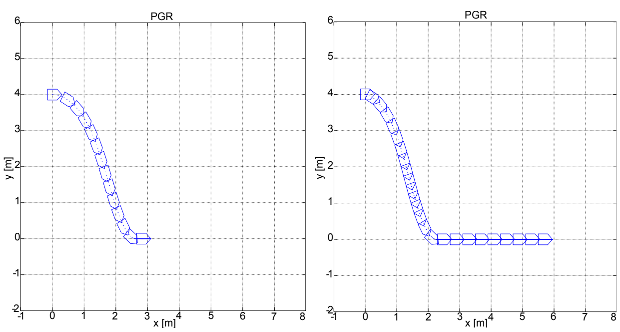

Fig. 4. **Example trajectories of the robot. Left by $u_1^{stb\_sig}$ and right by u_1 in (22).**

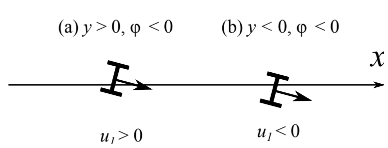

Fig. 5. **Back-and-forth phenomenon around x-axis using $u_1^{stb\_sig}$.**

As shown in Fig.5 using $u_1^{stb\_sig}$, in condition (a), according to the requirement of stability $u_1 > 0$, the robot continues to move forward. However, when it cross the x-axis, the state of the robot changes to condition (b) immediately. As the sign of y changes, the robot begins to move backward and turn into condition (a) again. The robot is trapped into the repeats of conditions (a) and (b). The control law u_1 in (22) can avoid this kind of phenomenon

E. Some Extensions for Modified Applications

If the mobile robot is moving in a straight line other than the center of the passage, we can modify the positions of the walls with the settings of $y = W_l$, $(W_l > 0)$ and $y = -W_r$, $(W_r > 0)$. Then, we can replace W in the control law with W_l when $y > 0$ and W_r when $y < 0$.

If we want to control the robot to move in reverse with tracking the negative direction of the x-axis, we can apply the following curves shown in Fig.6 in path function definition. In the region between the x-axis and $y = W$, the following

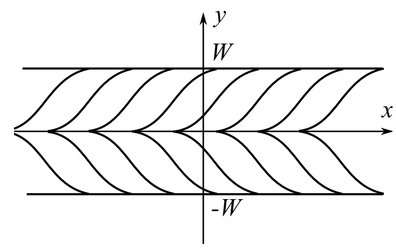

Fig. 6. **Coordinate system of the pathway for moving in reverse.**

curves which towards the x-axis are used.

$$y = \begin{cases} 0 & (x < \frac{-\pi+b}{a}) \\ \frac{W}{2}(1+\cos(ax-b)) & (\frac{-\pi+b}{a} \leq x \leq \frac{b}{a}) \\ W & (\frac{b}{a} < x) \end{cases} \tag{23}$$

$$\phi_r = \tan^{-1}\left(a\sqrt{(W-y)y}\right) \tag{24}$$

$$u_2 = \begin{cases} -\lambda_1 \phi & (|y| < \epsilon, |y| > W - \epsilon) \\ -\lambda_1 \left\{ \phi - \tan^{-1}\left(a\sqrt{(W-y)y}\right) \right\} & \\ \quad + \frac{a(W-2y)\sqrt{(W-y)y}}{2y[1+a^2(W-y)y](W-y)} \sin(\phi) u_1 & (otherwise) \end{cases} \tag{25}$$

As to the region between $y = -W$ and x, the signs of y need to be inverted in (25).

IV. Numerical Simulations and Experiments

In order to examine the property and efficiency of the extended PGR, we carry out simulations and experiments under three different conditions.

A. Experimental Equipment

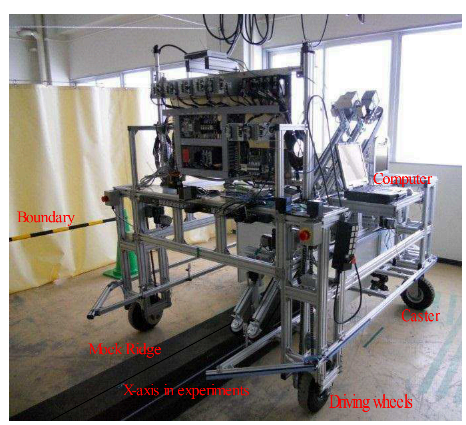

Fig. 7. **Equipment employed in the experiment.**

Fig.7 shows the mobile robot employed in the experiments. The robot is developed for agricultural harvest. Two front wheels are driven by motors and two rear wheels are casters. The wheel base is 1560 mm and the axle track is 1500 mm. The shape is like a gantry. The robot travels straddling a ridge. The experiment is performed in a passage indoor. Objective of the control is to make the center of the axle of the front wheels track to the central line of the mock ridge. The length of the mock ridge is 7 meters in x-direction. All the parameters and initial values of the experiments are the same with those of simulations.

To compare with the proposed PGR and show the property, a method of feeding back the lateral deviation and heading deviation is used[18]. To apply the deviation feedback method, we take the x-axis as target path and let the mobile robot advance in the positive direction. Set the lateral deviation as ξ and the orientation deviation as d. As shown in Fig.8, if the position coordinates of the mobile robot is set as (x, y), the azimuthal angle as ϕ, we can have $d = -y$ and $\xi = -\phi$. The control law can be presented by the following expression.

$$u_1^{cnv} = V_m \tag{26}$$

$$u_2^{cnv} = -k_d y - k_\xi \phi \tag{27}$$

In the rest of this paper, we refer to this control method as conventional method.

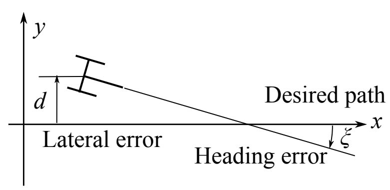

Fig. 8. **Lateral error and heading error.**

B. Three Prepared Conditions for Experiments

We prepare three sets of experimental conditions called CASE A, B and C. In CASE A, the robot starts from the position with 2 meters offset from x-axis. Parameters of the control is determined so that the robot converges to x-axis in around 4 meters for x coordinate. It is used as a standard setting in the following simulations and experiments. In CASE B, the initial angle of the robot body axis ϕ is changed with $\frac{\pi}{2}$ radian. All other parameters are set to the same values with CASE A. In CASE C, a disturbance with constant value is added to u_2 to find out the influences of disturbance on both control methods.

C. CASE A: Standard Setting

1) Simulation: The control parameters for the proposed PGR are set as $W = 3$, $a = 0.5$, $\lambda_1 = 0.7$, $\epsilon = 10^{-6}$, $c = 1$, $K_m = 1$, $c_m = 1$ and $V_m = 1$. The feedback gains of the conventional method are set as $k_d = 0.5$, $k_\xi = 1$. When the initial values are set as $x = 0$, $y = 2$ and $\phi = 0$, each trajectory of the robot is shown in Fig.10 and the time responses of the state are shown in Fig.11.

From Fig.10 it is obtained that robots controlled by conventional control and the proposed PGR have almost the same trajectories. Both of them reaches the x-axis around $x = 4$. From Fig.11, speed of the conventional method is faster than the proposed PGR from 0 second to 8 seconds. It is considered that the magnitude of u_1 of the proposed PGR tends to be smaller than the conventional method in the period when the robot is away from x-axis due to the term $e^{-c_m y^2}$ in (22). Around 8 seconds, ϕ of the proposed PGR changes quickly. It might be happen since $e^{-c_m y^2}$ approaches 1 and u_1 takes V_m.

2) Experiment: In Fig.11, the red line shows the trajectory of the robot controlled by the conventional method and the green line by the proposed PGR. Due to the limitation of the

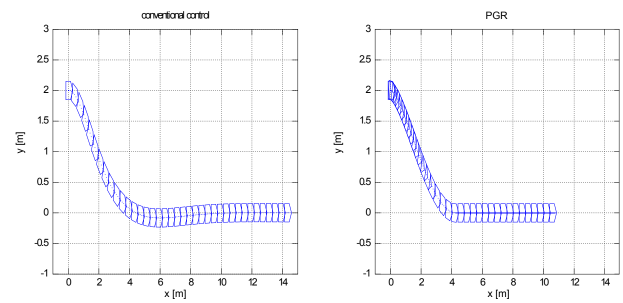

Fig. 9. **Trajectory of the robot in CASE A simulation. Left by the conventional control and right by the proposed PGR.**

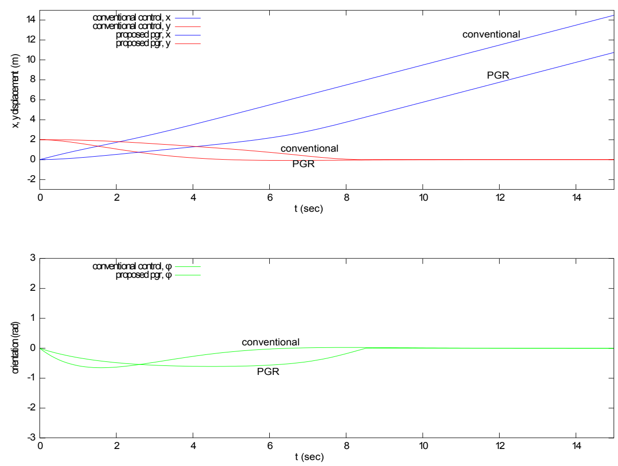

Fig. 10. **Time responses of x,y and ϕ in CASE A simulation. Both graphs of the conventional control and the proposed PGR.**

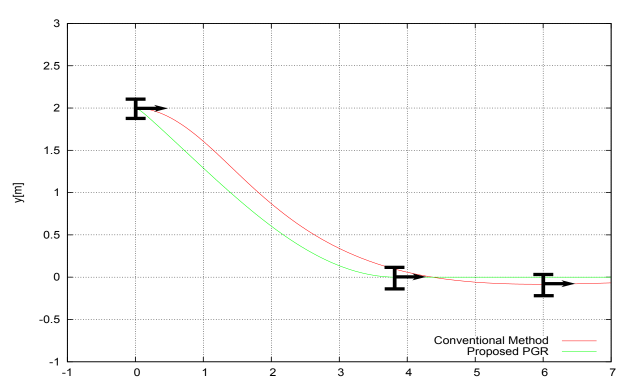

Fig. 11. **Trajectories of the robot controlled by conventional method and proposed PGR in CASE A experiment.**

motor power, we set V_m as $V_m = 0.1$. All other parameters are same as the simulation. We can see from the figure that the trajectory in the experiment is almost the same with that in simulation. It seems that the robot does not converge to x-axis in the conventional method. However, if we were able to continue the travel motion more than 10 meters, it would be achieved.

3) Discussion: By adjusting the parameters we can obtain almost the same trajectories controlled by the conventional method and the proposed PGR as the standard setting. Since the proposed PGR is designed to follow the path functions, it is easier to adjust the parameters than the conventional method.

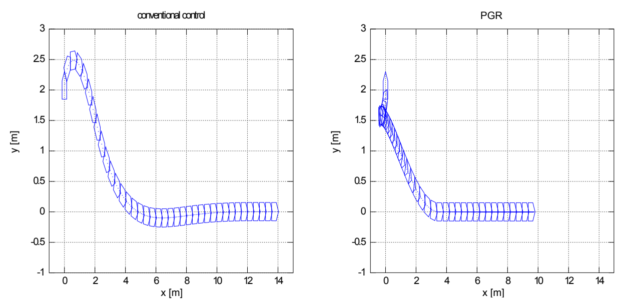

Fig. 12. **Trajectory of the robot in CASE B simulation. Left by the conventional control and right by the proposed PGR.**

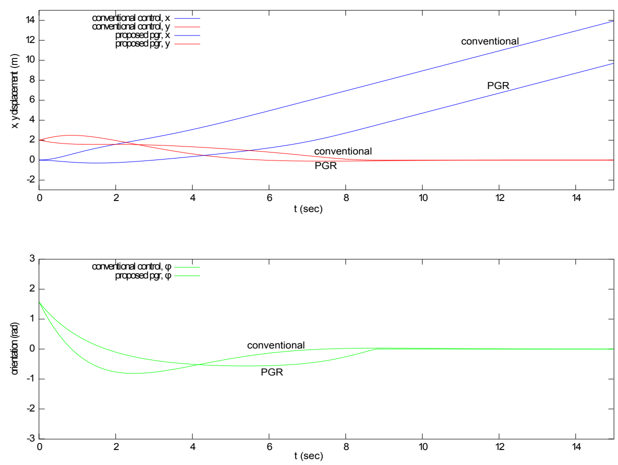

Fig. 13. **Time responses of x,y and ϕ in CASE B simulation. Both graphs of the conventional control and the proposed PGR.**

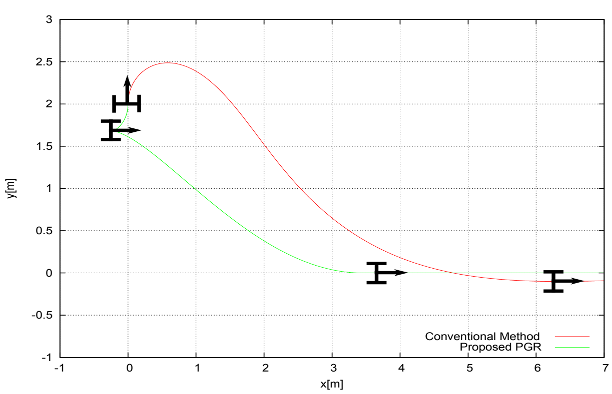

Fig. 14. **Trajectories of the robot controlled by the conventional method and the proposed PGR in CASE B experiment.**

D. CASE B: Change of The Initial Angle

1) Simulation: The initial angle is set as $\phi = \frac{\pi}{2}$. All the other parameters are kept as same as those in CASE A. Trajectories of the robot are shown in Fig.12 and the time responses of the state shown in Fig.13.

As shown in Fig.12, the robot controlled by the conventional method advances from $y = 2$ directly, changing its direction angle from $\frac{\pi}{2}$ to $-\frac{\pi}{2}$ gradually and then approach to the x-axis with overshoot action. It finally settles to x-axis until the x-coordinate of the robot has already been around 10 meters. On the other hand, the robot controlled by proposed PGR shows the cutting-the-wheel motion as explained in Fig.3. It settles to the x-axis when the x-coordinate is only around 3 meters.

2) Experiment: Experimental result is shown in Fig.14. The trajectories are almost same as those of the simulation. We can see from the experiment that the robot controlled by the conventional method moved forward for about 0.5 meters in y-direction after it started from the initial position and reached the x-axis around 5 meters. While the robot controlled by the proposed PGR moved backward for about -0.25 meters in x-direction and settled to the x-axis around 3 meters.

3) Discussion: Although both two methods can convergence to the x-axis successfully, convergence of the PGR is earlier than the conventional control. Meanwhile, when the robot starts near the walls, the strategy of moving backward firstly adopted by proposed PGR can avoid the possibility of collision with the boundaries which exists obviously in the conventional method.

E. CASE C: Applying Disturbance to u_2

1) Simulation: In CASE C, all the parameters and initial values are set to the same as CASE A. The only difference is that a disturbance with the constant value of 0.1 is added to u_2. The trajectories and time responses are shown in Fig.15 and Fig.16 respectively.

We can see from the figures that there is a deviation of about 0.2 meters from the x-axis with conventional method. On the other hand, the deviation is only about 0.05 meters with proposed PGR.

2) Experiment: Experimental result is shown in Fig.17. After $x = 4$ meters the robot controlled by the proposed PGR continue to approach the x-axis while the robot controlled by the conventional method become parallel with the x-axis. Finally, the deviations are about 0.2 meters and 0.05 meters by the conventional method and the proposed PGR respectively. Although we set the value of ϵ to 10^{-6}, the deviation is lager than this value due to the influence of the disturbance.

3) Discussion: The results of simulation and experiment shows that the deviation of PGR is smaller than that of the conventional control. The reason is considered as follows. $\phi = 0$ is satisfied when both the proposed PGR and the conventional control are in steady-state. Then $u_2^{cnv} = -k_d y$ is obtained based on (27). This is a proportional control on y in which the feedback gain is k_d. The deviation can be reduced by taking strategy of increasing the value of k_d. However, the trajectory of the robot may suffer from the strategy. As to the proposed PGR, $u_2 = \lambda_1 \phi_r$ is obtained based on (14) when $\phi = 0$. As u_2 is a nonlinear function of y, we linearize it around $y = 0$. Then we obtain $u_2 \approx -k_y y$ where $k_y = -\lambda_1 \frac{\partial \phi_r}{\partial y}$. According to (10), $k_y \to \infty$ when $y \to 0$. Therefore, it becomes a high gain feedback when y becomes smaller. This is considered as the reason that the steady-state error of y in proposed PGR becomes smaller.

F. Control Performances under Different Initial Poses

To show the relationship between the initial pose of the robot and the control performance of the proposed PGR, some supplementary simulations are performed. All the parameters are set to the same as CASE A. Trajectories of the robot are shown in Fig.18, through which the proposed PGR shows its applicability and ability to keep its tracking features under different initial poses.

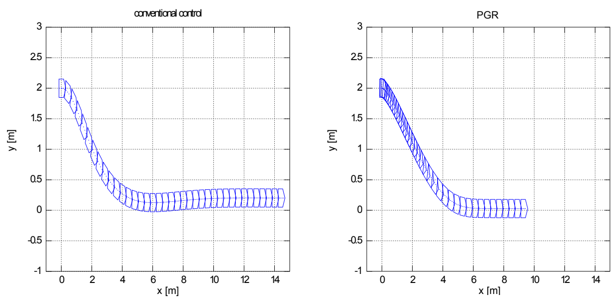

Fig. 15. **Trajectory of the robot in CASE C simulation. Left by the conventional control and right by the proposed PGR.**

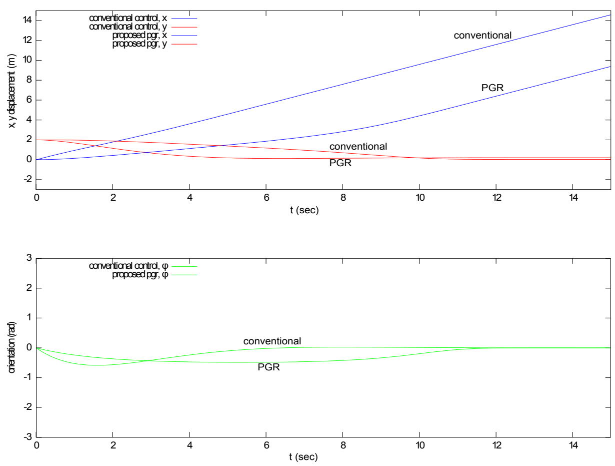

Fig. 16. **Time responses of x,y and ϕ in CASE C simulation. Both graphs of conventional control and proposed PGR.**

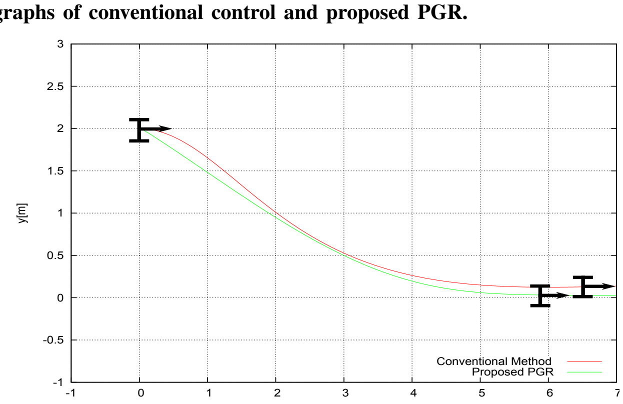

Fig. 17. **Trajectories of the robot controlled by conventional method and proposed PGR in CASE C experiment.**

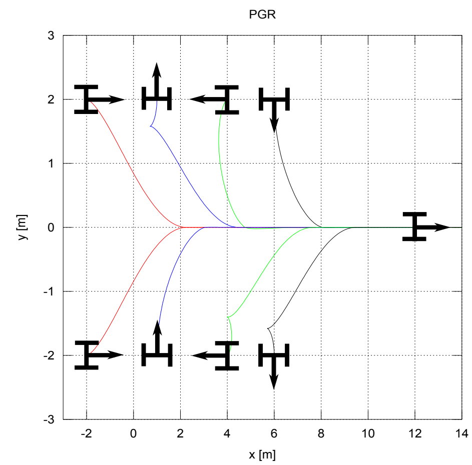

Fig. 18. **Trajectories of the robot controlled by proposed PGR under different initial poses.**

V. CONCLUSIONS

Path-generating regulator along a straight passage is a new control method for the two-wheeled non-holonomic mobile robots. According to our research, this method has shown its superiority and applicability in solving the tracking problem along a straight passage in simulations and experiments. Its tracking features can avoid the possibility of collision with boundaries of passage successfully and the ability of removing external disturbance with constant values is stronger compared with the conventional control. We also shows the tracking performance under the constant disturbance. In future work, we will carry out a further research on the path-generating regulator along a curve passage.

VI. ACKNOWLEDGMENT

This work was partially supported by a sponsored research project with CS Solution Incorporated.

REFERENCES

[1] M. Sampei, Feedback Control of Nonholonomic Systems, *Journal of the Society of Instrument and Control Engineers*, Vol.39, No.6, 1997, pp.396-403.

[2] R.W. Brockett, Asymptootic Stability and Feedback Stabilization, *Differential Geometric Control Theory*, 1983, pp.181-191.

[3] R.M. Murray, S.S. Sastry, Steering nonholonomicsystems in chained form, *Proc. of the 30th IEEE Conference on Decision and Control*, Vol.2, 1991, pp.1121-1126.

[4] B.L. Ma, S.k. Tso and W.L. Xu, Adaptive/Robust Time-Varying Stabilization of Second-Order Nonholonomic Chained Form with Input Uncertainties, *International Journal of Robust and Nonlinear Control*, 2002.

[5] O.J. Sordalen and O. Egeland, Stabilization of Nonholonomic Systems by discretization, *Proceedings of IFACWorld Congress*, 1993.

[6] H. Khennouf and C.C.de Wit, Quasi-Continuous exponential stabilizers for nonholonomic systems, *Proc.of 13th IFAC World Congress*, 2b, 174, 1996, pp.49-54.

[7] A. Astolfi, Discontinuous control of Nonholonomic Systems, *System and Control Letters*, Vol.27, 1996, pp.37-45.
[8] N. Marchand and M. Alamir, Discontinuous exponential stabilization of Chained Form Systems, *Automatica*, Vol.39, No.2, 2003, pp.343-348.
[9] M. Sampei, A control strategy for a class of nonholonomic systems - time-state control form and its application, *Proceedings of the 33rd IEEE Conference on Decision and Control*, vol.2, 1994, pp.1120-1121.
[10] J.A. Primbs, V. Nevistic and J.C. Doyle, Nonlinear Optimal Control: A Control LYAPUNOV Function And Receding Horizon Perspective, *Asian Journal of Control*, Vol.1, No.1, 1999, pp.14-24.
[11] A. Takashima, Y. Hashimoto, K. Hori, N. Hanajima, H. Hikita and M. Yamashita, Feedback control of Non-holonomic Mobile Robots by Path-generating Regulator, *Transactions of the Japan Society of Mechanical Engineers - Part C*, Vol.70, No.689 (2004), pp.120-126.(In Japanese)
[12] N. Hanajima, A. Takashima, H. Hikita and M. Yamashita, Path-generating Regulator with SLAM for Navigation of Two-wheeled Mobile Robots, *39th International Symposium on Robotics 2008*, 2008, pp.227-231.
[13] N. Kondo, M. Monta, Fruit Harvesting Robotics , *Journal of Robotics and Mechatronics*, Vol.11, No.4, 1999, pp.321-325.
[14] Y. Kawaguchi, I. Yoshida, H. Kurumatani, et al, Internal pipe inspection robot, *Proceedings of IEEE International Conference on Robotics and Automation*, vol.1, 1995, pp.857-862.
[15] N. Hanajima, Path-generating Regulator for a straight Passage, *Private Report*, 2012.(In Japanese)
[16] Y.J. Kanayama and F. Fahroo, A new line tracking method for nonholonomic vehicles, *Proceedings of IEEE International Conference on Robotics and Automation*, vol.4, 1997, pp.2908-2913.
[17] Y. Kanayama, Vehicle Path Specification by a Sequence of Straight Lines, *IEEE Journal of Robotics and Automation*, vol.4, no.3, 1988, pp.265-276.
[18] N. Kondo, S. Noguchi and M. Monta, Agricultural Robot (1) Fundamentals and Theory, *Corona Publishing* , TYO, 2004.(In Japanese)